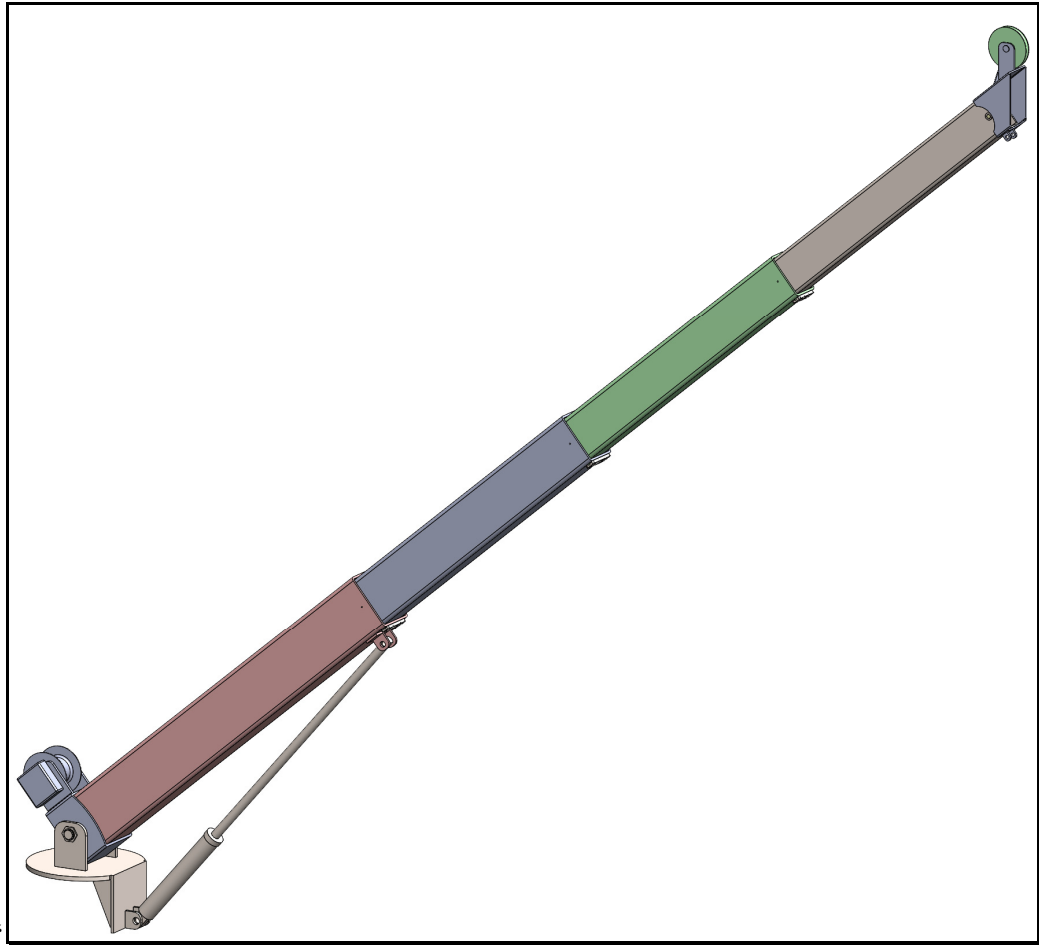


Proposed Reach Boom:  
Structural Simulation and  
Performance Tabulation



*April, 2020*

Shawn Mahaney,  
Lead Analyst

## 1.0 Problem Summary

A telescoping crane boom design is proposed. The design uses standard steel sections and catalog hardware to make a low-cost light-capacity market entry. Final tube length and overlap schedules are to be determined. This study is performed to establish validity of the design concept and to better bracket the possible overlap/capacity combinations.

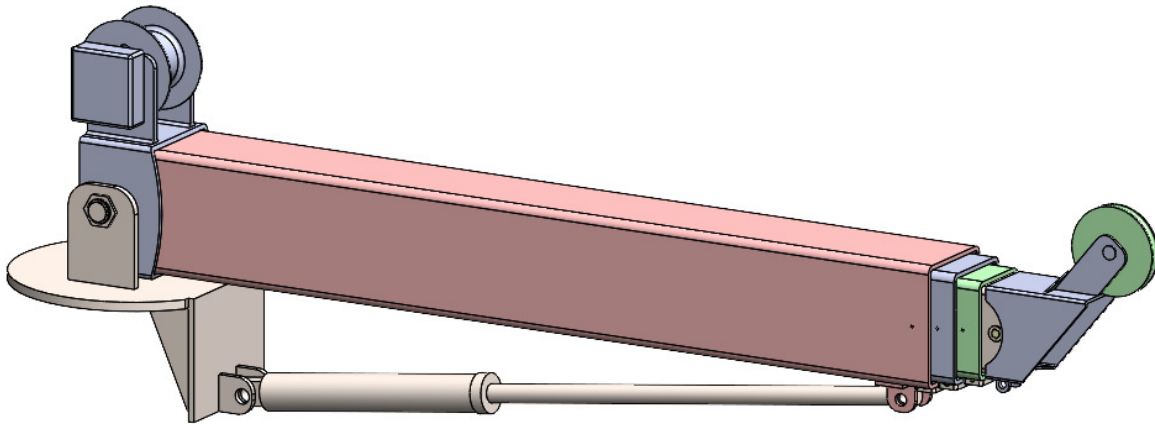


*Figure 1a – Retracted boom on simple support*

The boom is specified to have a 238 inch extended length, cable spool to front sheave, at 800 pound capacity. Retracted length and total weight is dependent on the chosen tube length. Target loaded extend/retract time is 75 seconds in either direction.

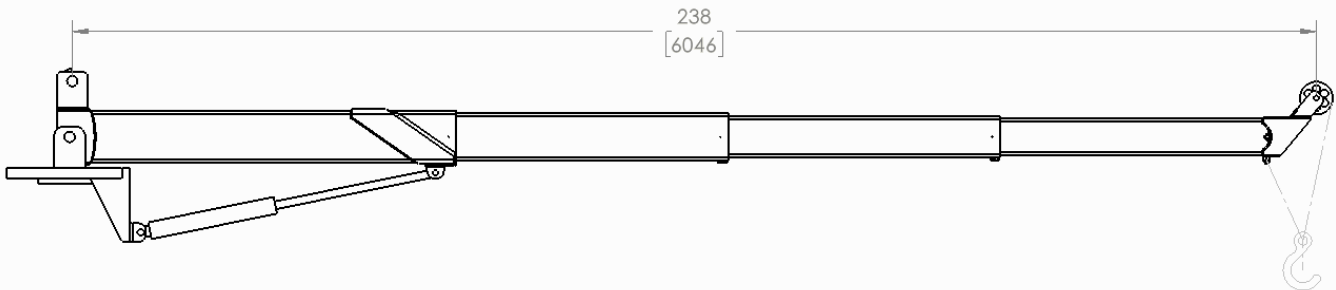


*Figure 1b – Extended boom with dimensions*

## 2.0 Design Details and Evaluation Criteria

There are four tubes in the boom. At each of the three overlaps there are two bolt-on cartridges each holding two roller bearings to take the primary loads. For lateral control there are four flat polymer wear pads each captive inside sets of weld-on bars. The wear pads are expected to be greaseable from inside the boom, through a retainer screw with integrated flush fitting. Both roller cartridges and wear pads are shimmable for build adjustment.

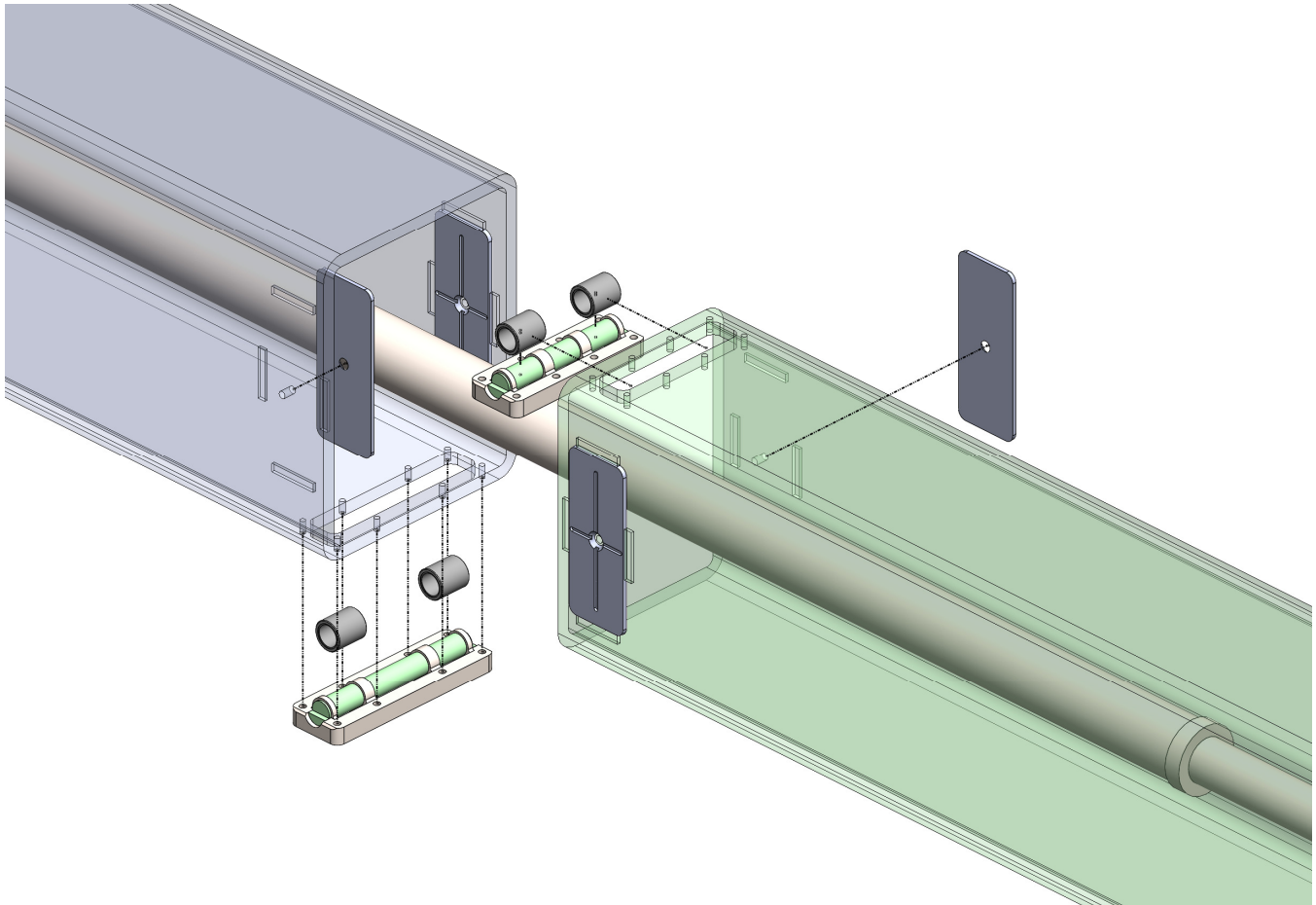


*Figure 2a – Exploded view of overlap with rollers and wear pads*

Each roller cartridge has a frame with eight bolt holes. This frame carries a shaft on which two rollers bearings ride. The shaft is keyed on both ends for location and anti-rotation relative to the tube section. The tube sections are planned to be made from a high-hardness variety of A513 carbon steel sections, wall thickness of  $\frac{1}{4}$  or  $\frac{3}{8}$  inch.

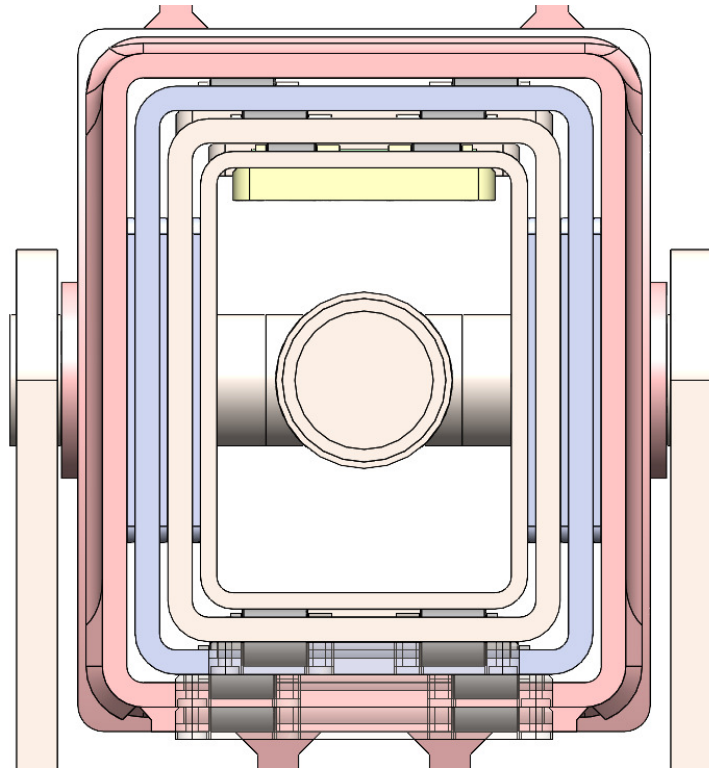


*Figure 2b – Section view showing tube sections*

Success of this design hinges on performance of the tube sections and the load-bearing hardware. The stated questions driving this analysis work are:

- Are stresses in the tube walls acceptable?
- Are loads in the rollers and pads under rated levels?
- Are stresses in the roller assemblies acceptable?

The assembly is to be studied carrying rated load, both static vertical and with a 15 degree lateral offset to accommodate swinging or misaligned loads.

### **3.0 Procedure**

A CAD model of the assembly was supplied in Solidworks format. A duplicate Solidworks model was made and modified for simulation work.

The model was configured at five different tube length and overlap values, for study of response in contact forces.

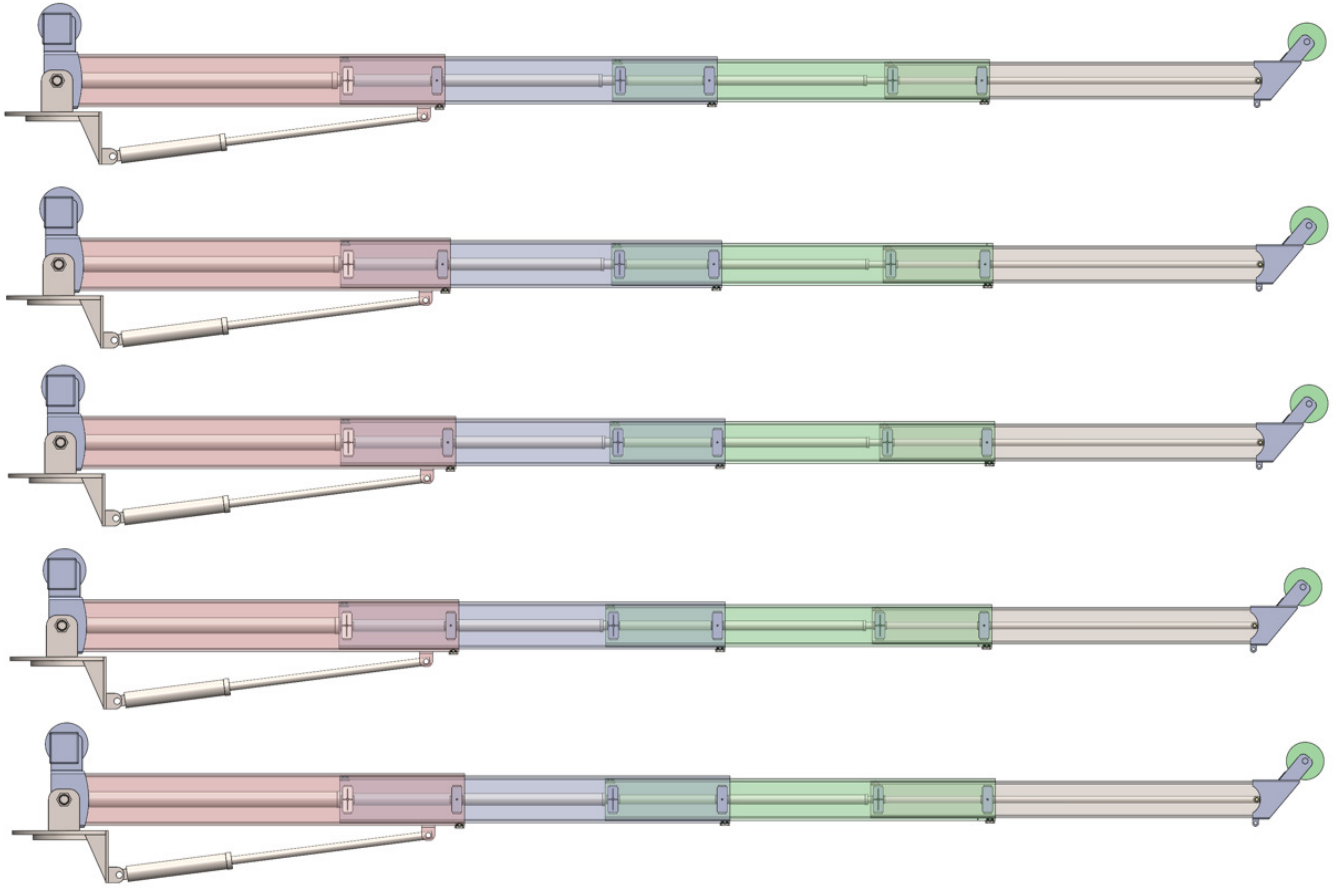
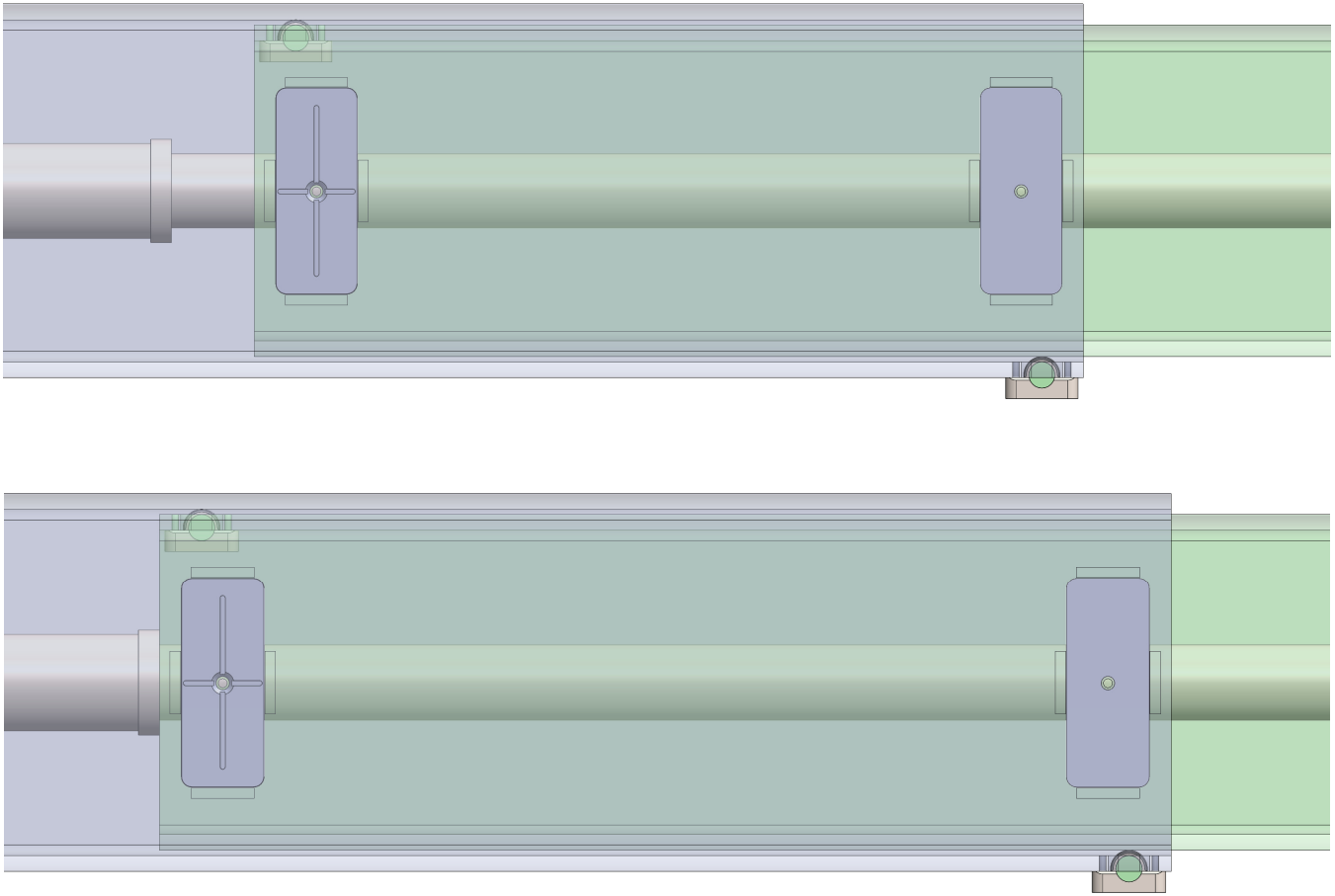


Figure 3a – Overlap configurations at contact extended length

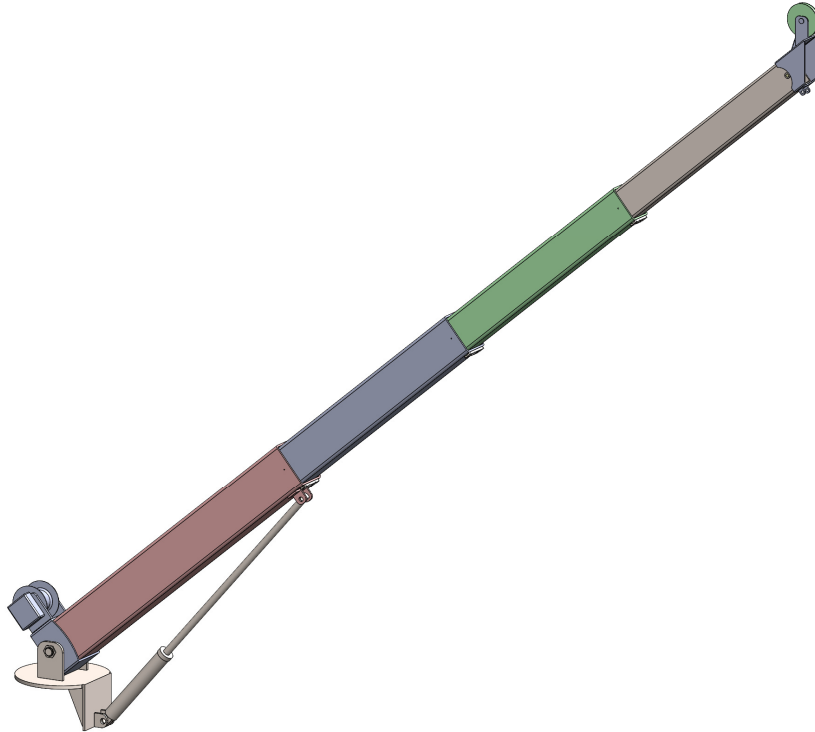
	<u>Retracted,</u> <u>drum-</u> <u>drum (in)</u>	<u>Extended,</u> <u>drum-</u> <u>drum (in)</u>	<b><u>section</u></b> <b><u>overlap</u></b> <b><u>(in)</u></b>	<b><u>roller</u></b> <b><u>overlap</u></b> <b><u>(in)</u></b>	<u>nominal</u> <u>section</u> <u>length</u> <u>(in)</u>	<u>mass of</u> <u>sections</u> <u>(lbm)</u>
baseline	88	238	20	18	72	783
plus1	88.8	238	21	19	72.75	791
plus2	89.6	238	22	20	73.5	99
plus3	90.3	238	23	21	74.25	807
plus4	91.1	238	24	22	75	815

Table 3b – Tabulation of basic dimensions



*Figure 3c – Tube overlap increase from 18 to 22 inches*

The boom is planned for elevations up to 55 degrees. The model is configured at 25, 40, and 55 degrees elevation for guidance in establishing a load rating chart.



*Figure 3d – Boom extended at 40 degree elevation*

For simulation the motor spool is replaced with a fixed axle, with a ‘wing’ shape that provides a vertex at the tangent point of the planned load cable. The hook end of the boom is modeled with a free-spinning body, split to make vertices at the tangent points of the load cable at each elevation.

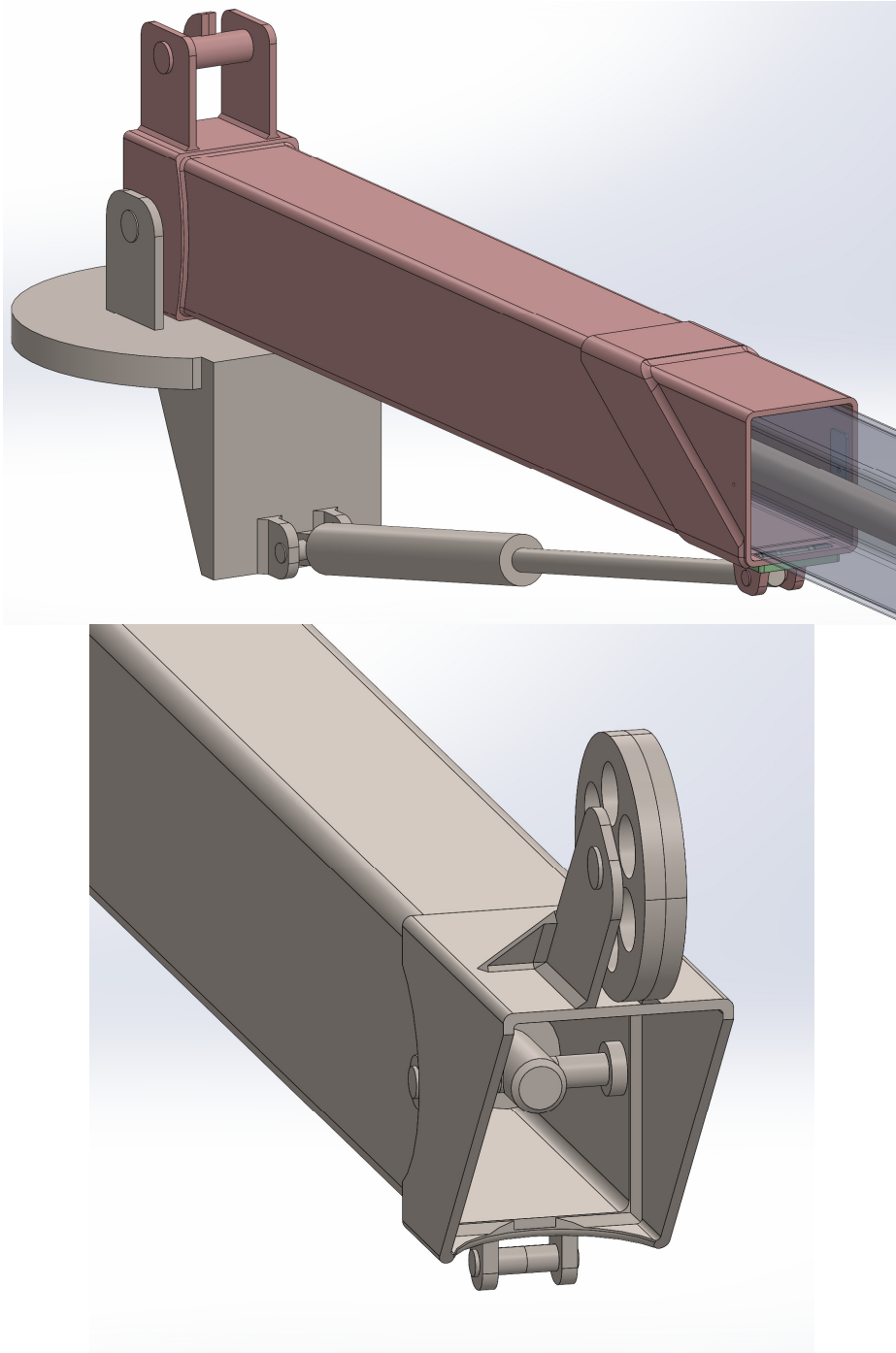


*Figure 3e – CAD models of motor and hook ends of boom assembly for simulation*

Both end sections of the boom are weldments. The welded parts are joined into a single solid, with weld beads modeled. Significant overlaps between welded parts are cut into the model as literal gaps.

After start of detail design work early studies showed need for a reinforcing band around the end of the first weldment. This band was added to the simulation model for the presented results.

The simple base model is fixed in space. Loading is by force vectors on the sheave tangent and static cable fixture, plus a gravity vector. The lift cylinder is modeled simply but literally in two pieces, length fixed as appropriate.

The proposed extension cylinder is a multi-stage double-acting model. For these studies it is replaced with a one-piece tube of correct approximate weight.

For the bulk of these studies it is assumed that the roller cartridge design and wear pad retention are successful, so the cartridges and wear pads are bonded to the main tubes. A later more detailed study is performed to validate the roller cartridge design.

All studies are linear static stress-strain simulations. Second-order finite elements and high accuracy contact are used. Details of the setup are in the appendix.

### 4.0 Results Summary

Studies performed are summarized in the following table. Complete force results are tabulated in the appendix.

STUDIES					
study	load angle	cut length	overlap	lift angle	load (lb)
A0	0	72	20	0	1600
A1	0	72.75	21	0	1600
A2	0	73.5	22	0	1600
A3	0	74.25	23	0	1600
A4	0	75	24	0	1600
B0	15	72	20	0	1600
B1	15	72.75	21	0	1600
B2	15	73.5	22	0	1600
B3	15	74.25	23	0	1600
B4	15	75	24	0	1600
C25	0	72	20	25	1732
C40	0	72	20	40	1990
C55	0	72	20	55	2550
C55-4	0	75	24	55	2550

*Table 4a – Summary of Studies*

“A” series studies are run with the boom horizontal, at full extension, and vertical load. Five configurations are run with different tube lengths and resultant overlap.

“B” series studies run the same geometry as series “A”, with the load vector at a 15 degree angle from vertical (to the operator right).

“C” series studies start with the boom geometry of study A0 elevated at three angles, 25, 40, and 55 degrees. The load is vertical and indexed according to a proposed load chart formula. An additional study at 55 degrees elevation is run with the boom geometry from study A4.

To illustrate force trends, values are taken from the second tube section (from operator end), on the operator left side rollers and pads.

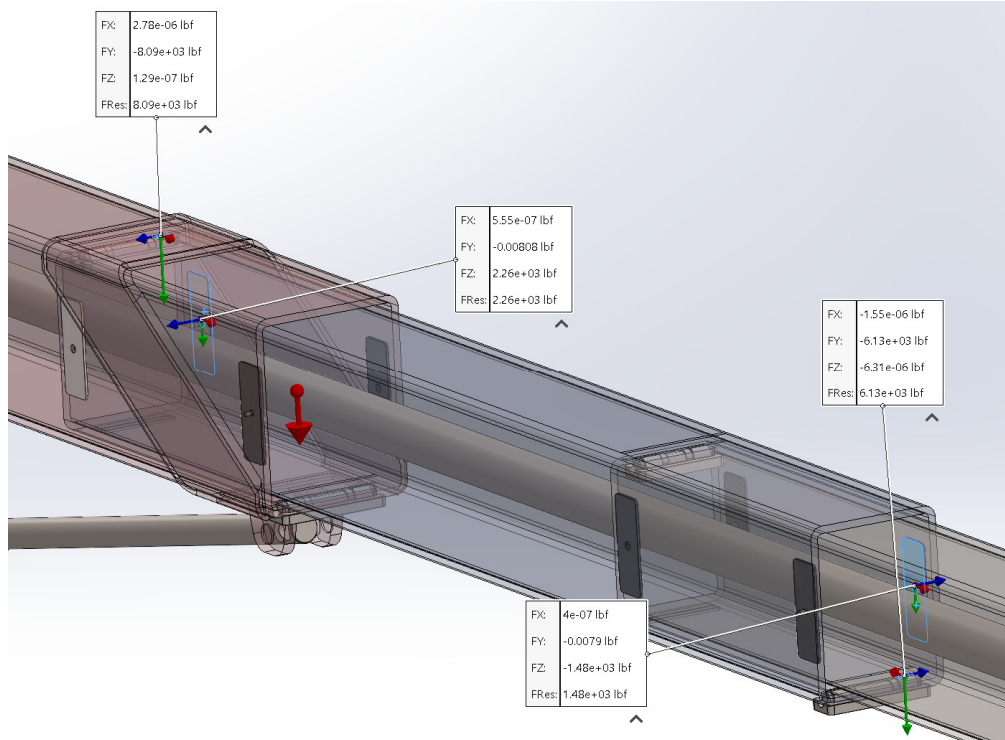


Figure 4b – Force probe locations

Forces on these locations are graphed over the “A” series of studies, vs tube length. Data are from the bearing cartridges bolted to tube 2, bearing on tubes 1 and 3.

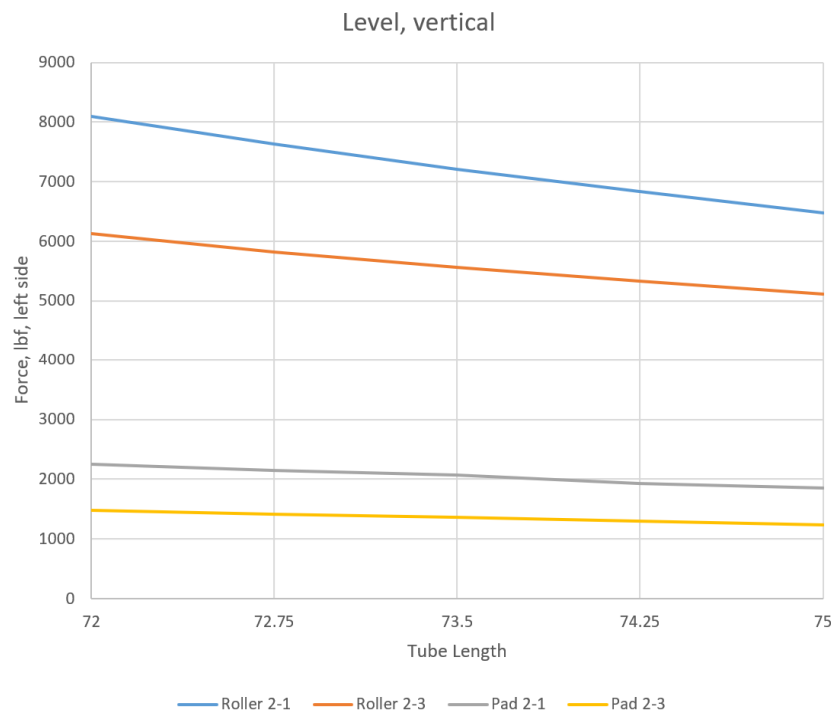


Figure 4c – Contact forces with level load

Forces drop predictably with increasing overlap.

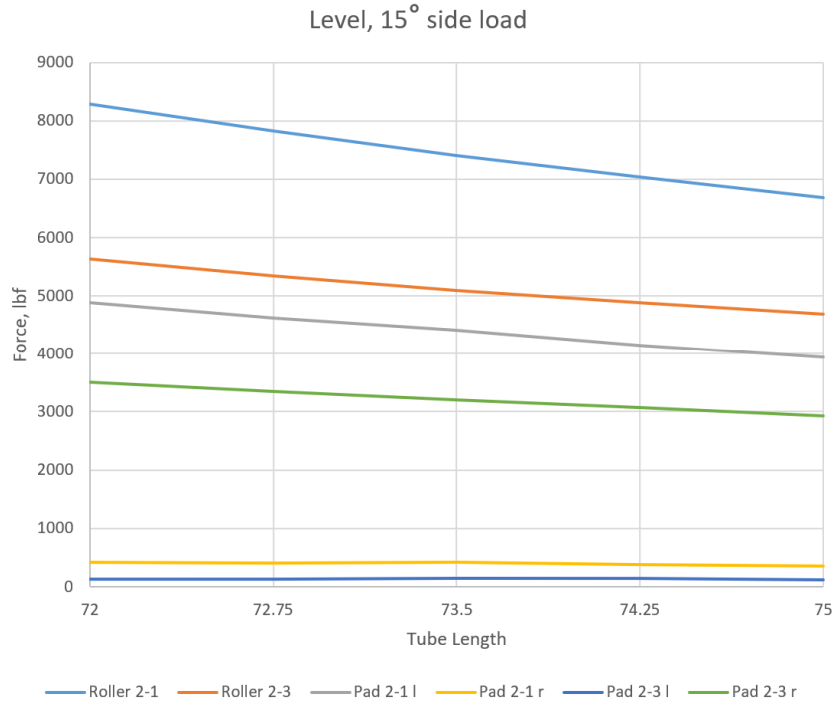


Figure 4d – Contact forces with lateral load

With lateral loading added, right side wear pads are included.

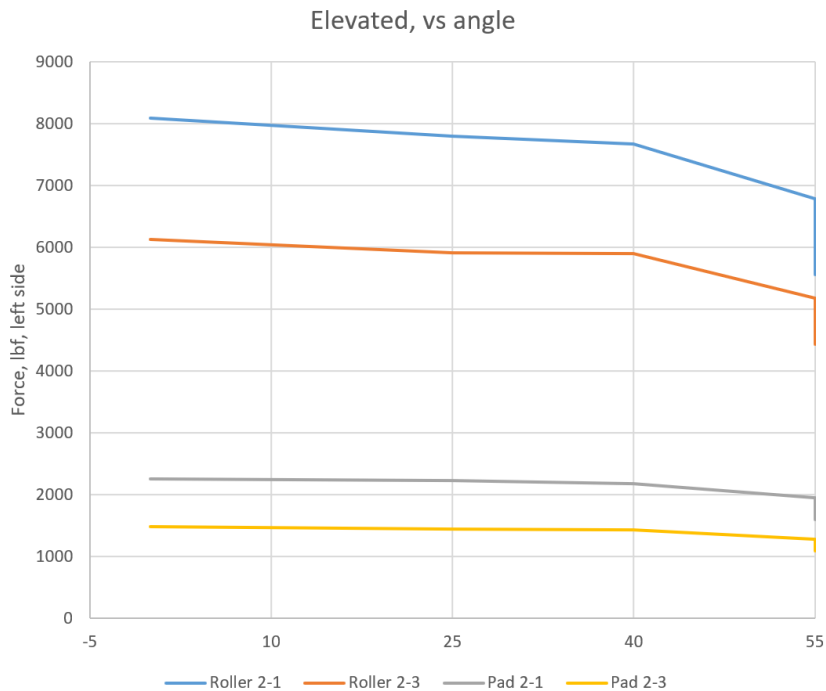


Figure 4e – Contact forces vs elevation

As the boom is elevated, forces decrease slightly. The load schedule formula is conservative. Note that the last elevation includes points for 75 and 72 inch tube lengths.

The static load rating of the main roller bearing is 6300 pounds force. A smaller bearing is used only at the position fixed to tube 4 where it bears on tube 3; this bearing is rated for 3700 pounds force.

In many of the studies the hardware load ratings are violated, not accounting for any factor of safety. In particular, the rollers between sections 1 and 2 are loaded over rating in most studies. At the worst the force acting on these rollers exceeds 9000 pounds. See appendix for a full tabulation.

The wear pads are rated for 2520 pounds normal force while sliding. In many cases this value is also exceeded.

Stresses in the tube sections are generally acceptable. Small hot spots can be noted at points of contact with the rollers. The stress field is most complicated where the lift cylinder supports the end of the first tube section.

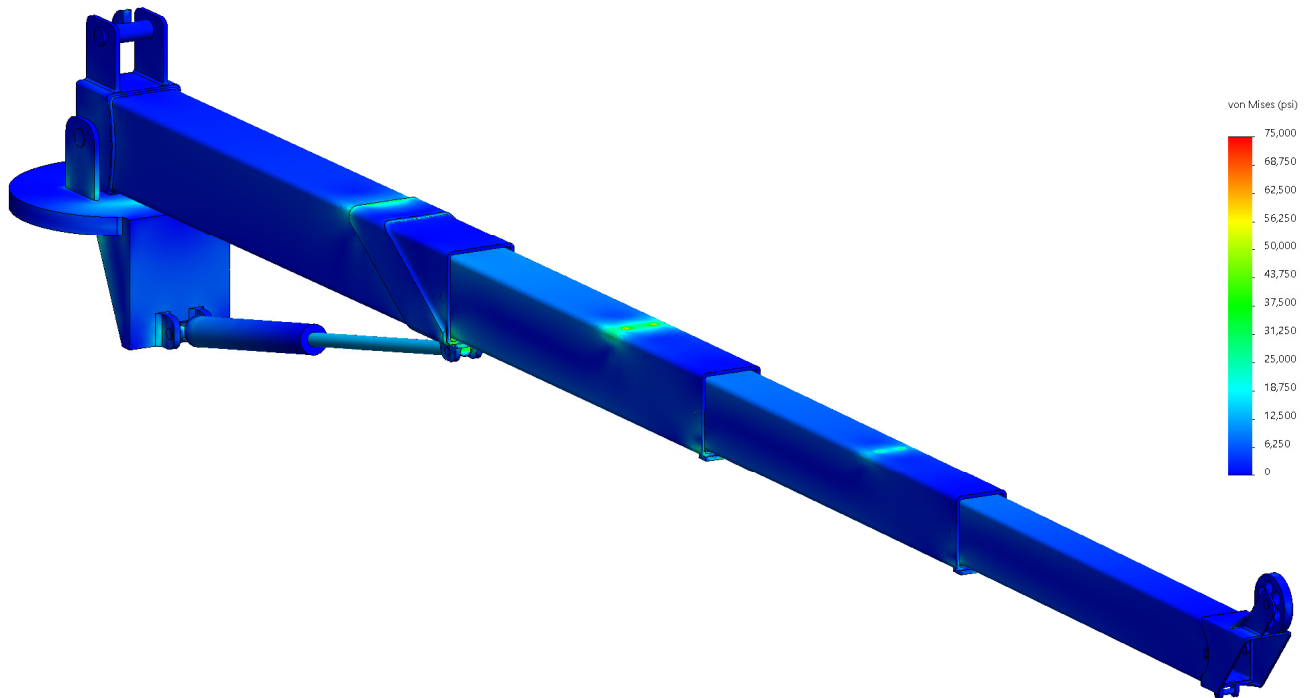


*Figure 4f – Surface stresses, level load, minimum overlap*

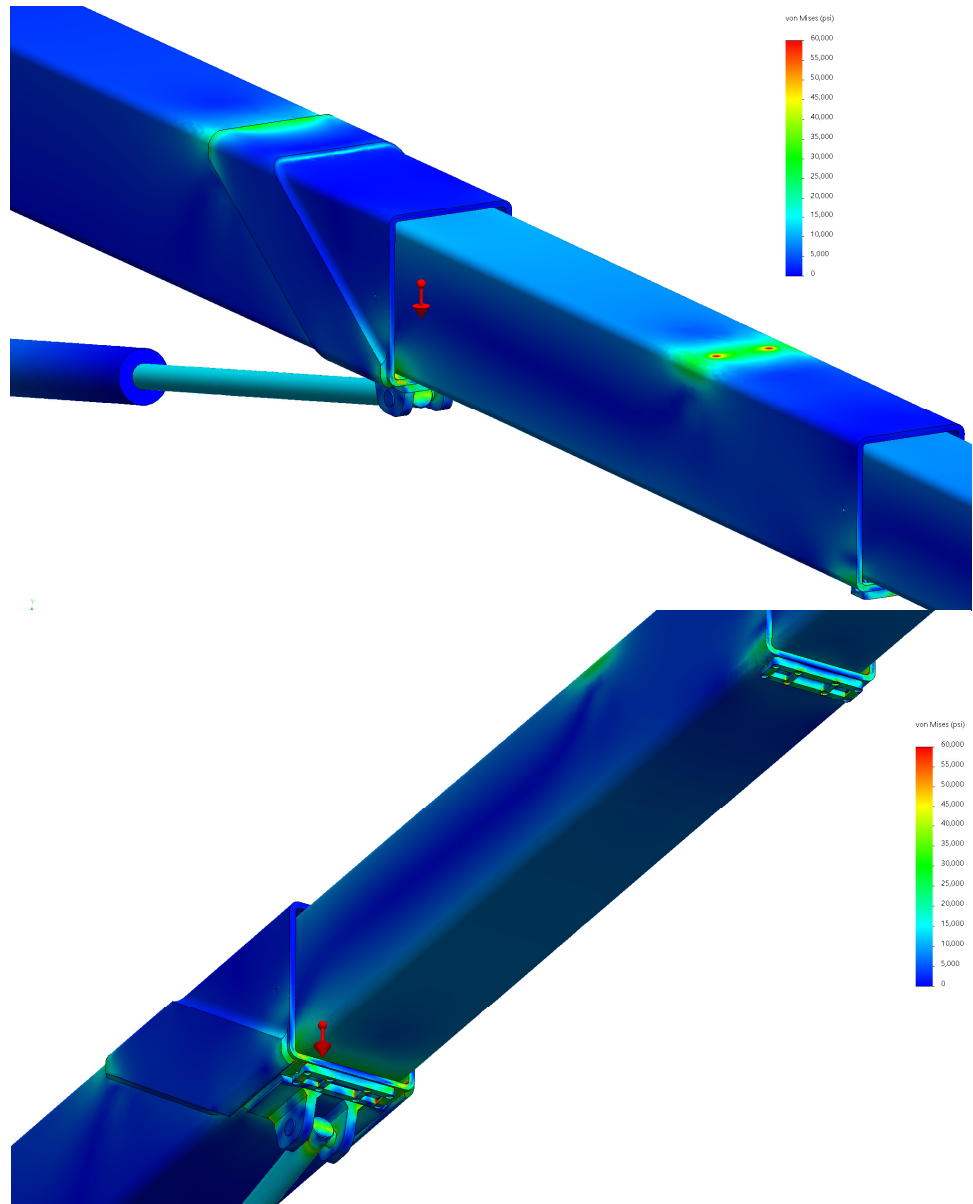


Figure 4g – Additional views of previous stress plot (60 ksi scale)

Vertical deflections are in the expected shape, 2.73 inches in the worst case (minimum overlap).

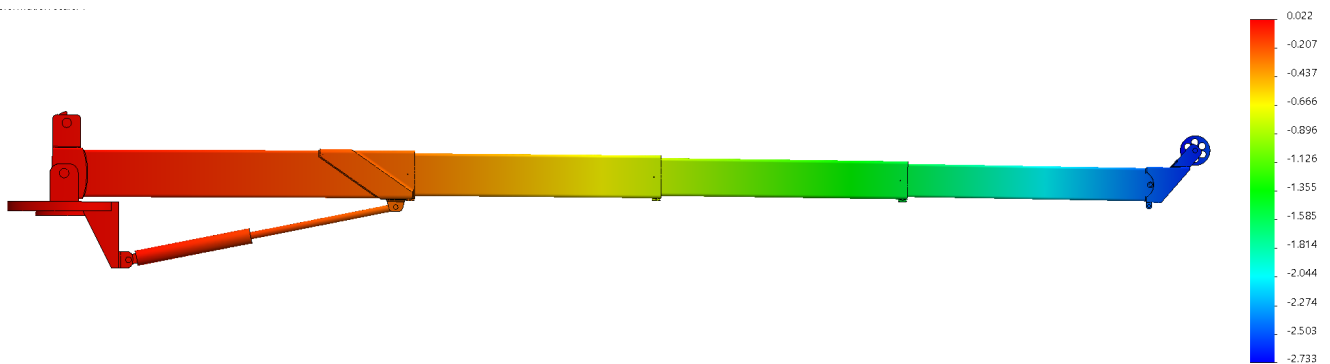
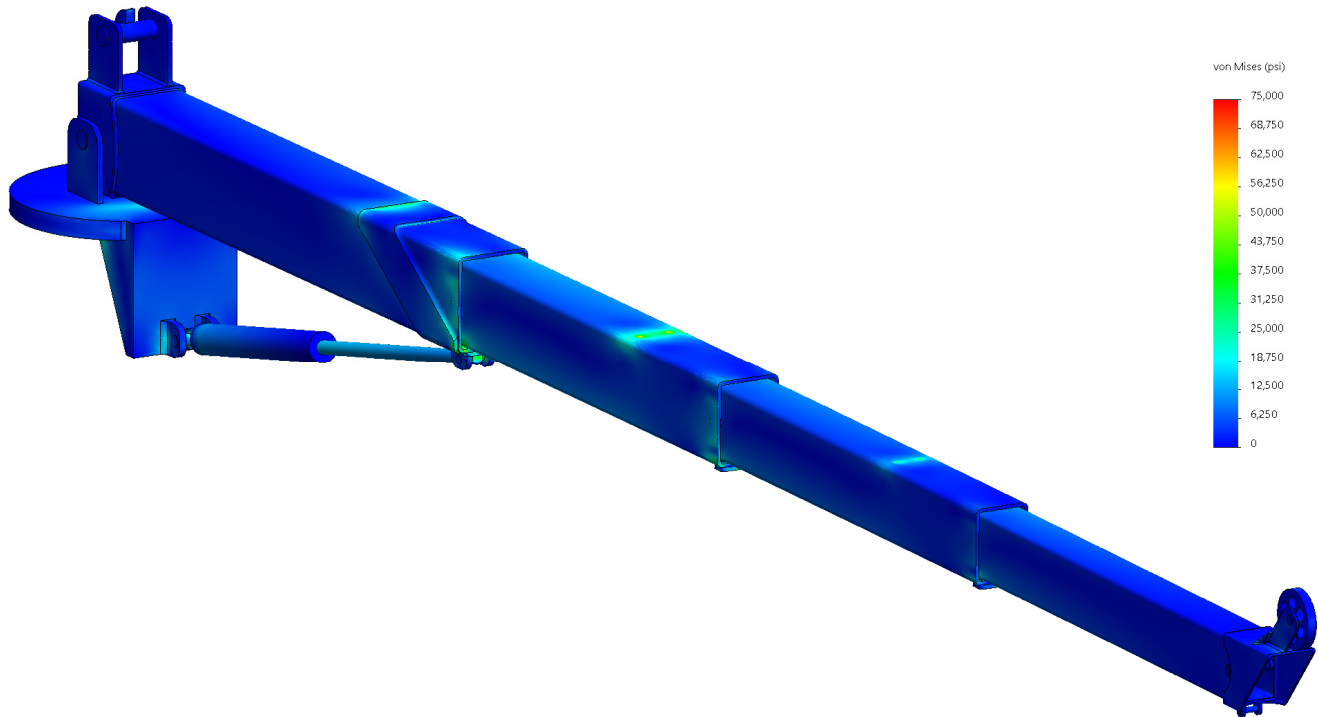


Figure 4h – Vertical deflection, level load, minimum overlap (blue down).

The stress pattern shows modest changes when the load is at a 15 degree angle. The following figure can be compared directly to the first stress plot.



*Figure 4i – Surface stresses, lateral loading*

As the boom elevation angle is increased, the proposed load chart conservatively reduces the primary bending moment of the load. Overall stress in the tube surfaces is seen to drop slightly.

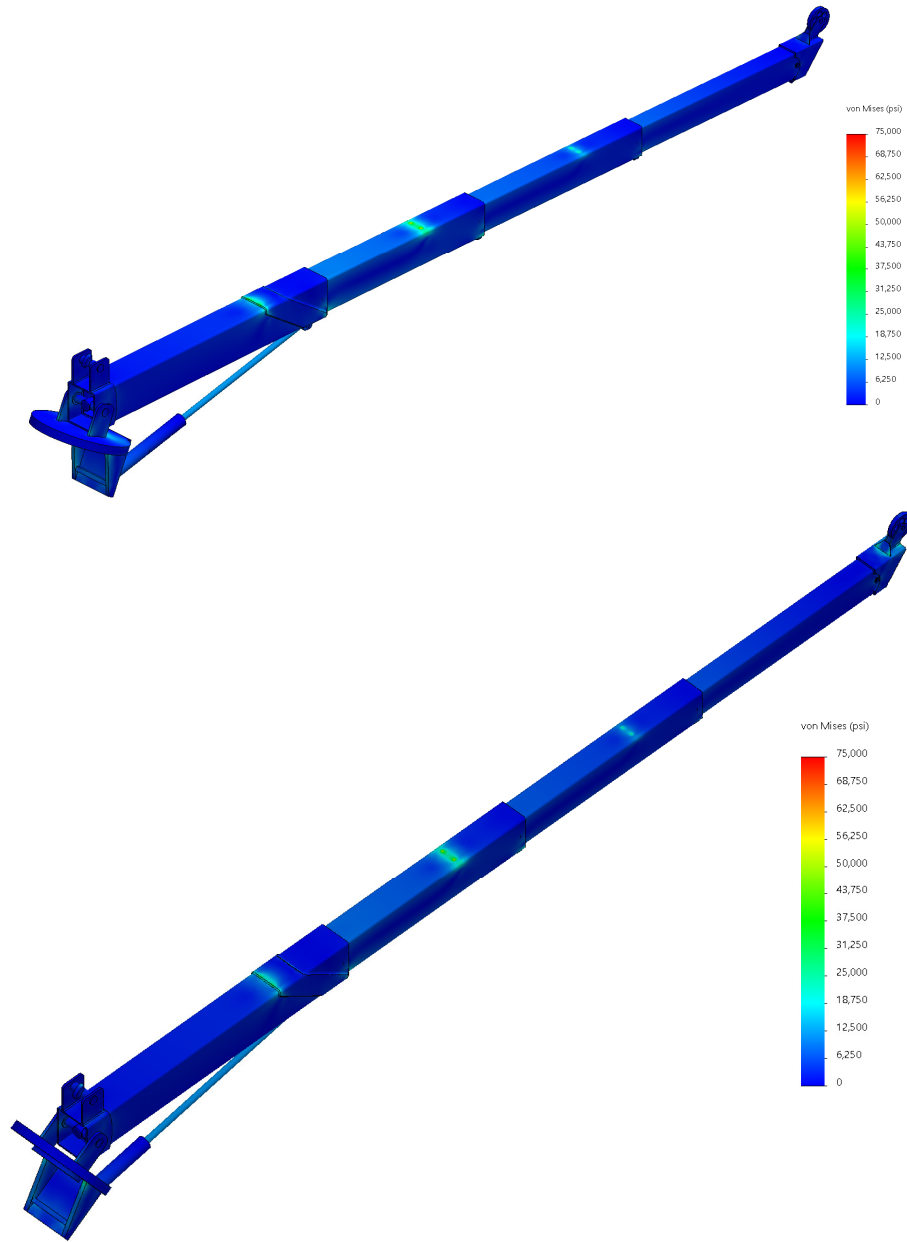


*Figure 4j – Surface stress with boom at 25 and 55 degrees elevation*

## 5.0 Detailed Analysis

Structural response in key areas was investigated in more detail.

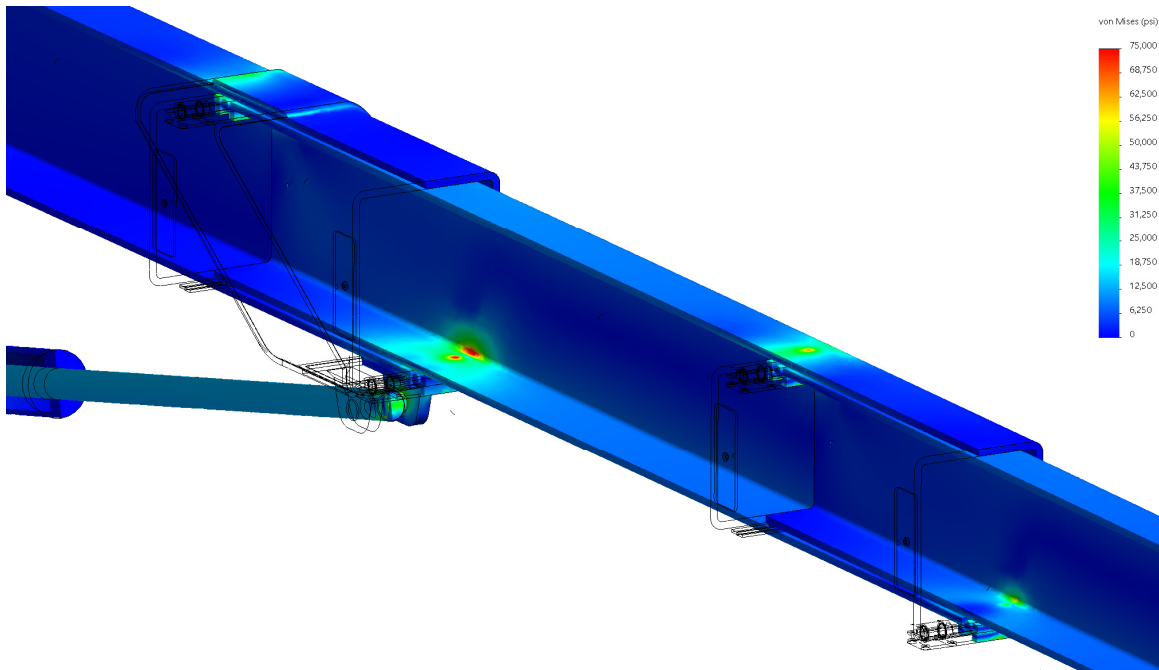


Figure 5a – Section through stress plot (level load, minimum overlap)

Early modeling work led to reinforcement of the outer end of tube #1. This area sees support from the lift cylinder introduced, inside the largest moment arm from bearing pairs. A reinforcing band was designed which fit over the original geometry, to be welded all around. For the simulation model a gap was maintained inside the band, it being joined only at the welds which were modeled in 3D. The mesh was refined to capture high gradients in this area.

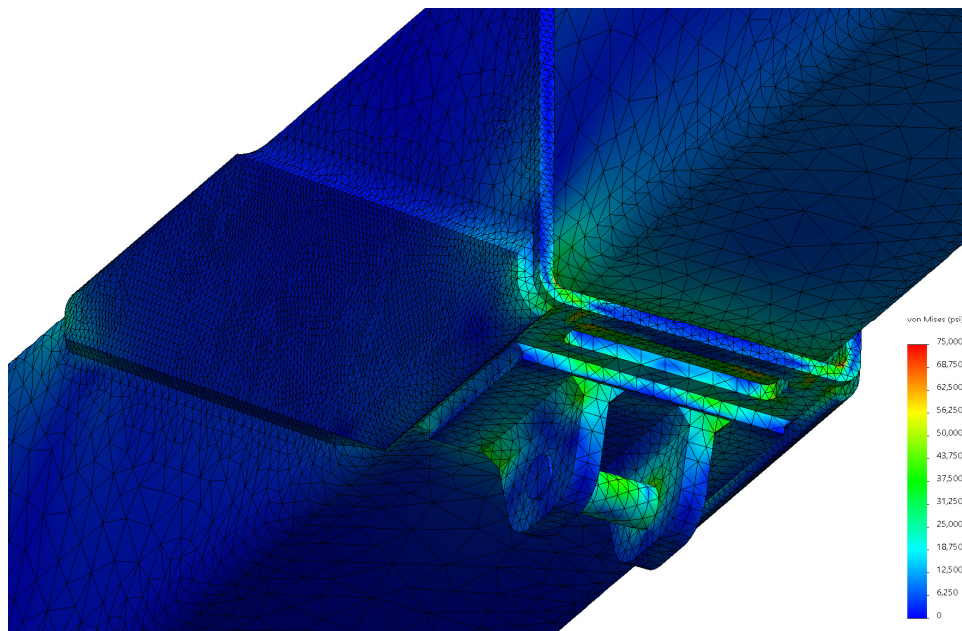
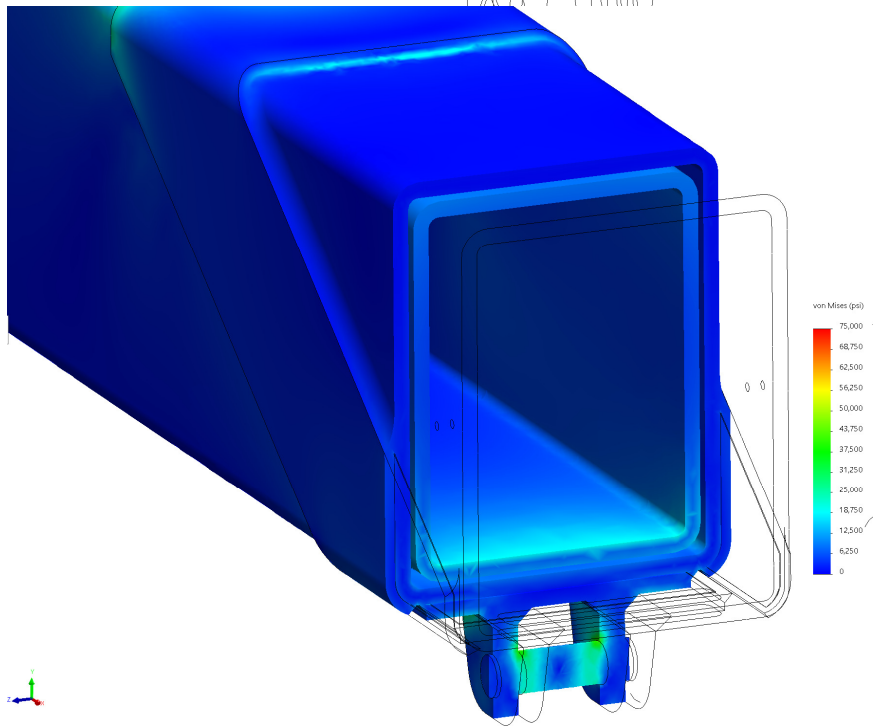
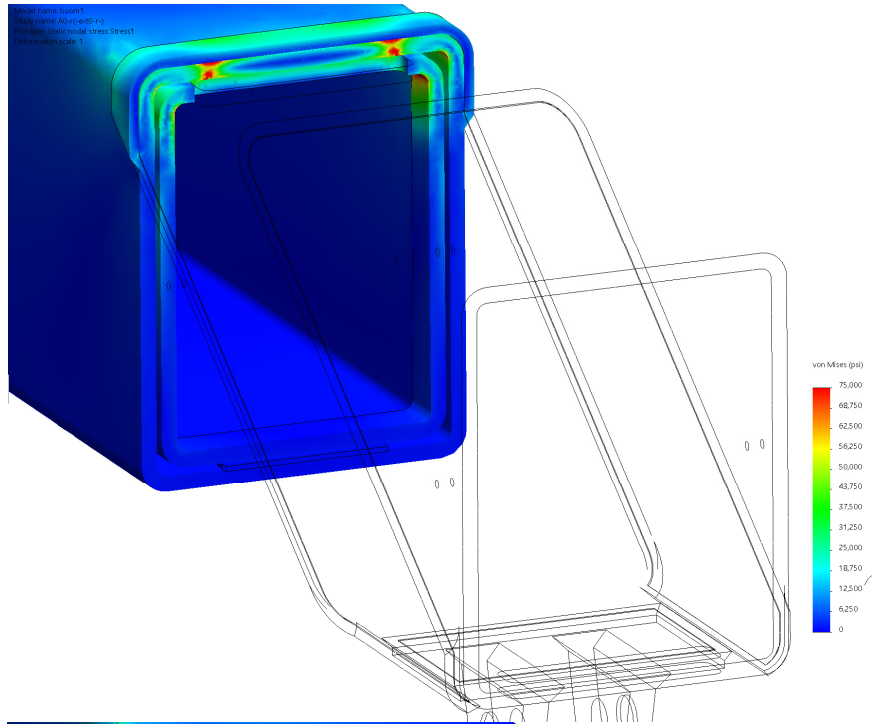
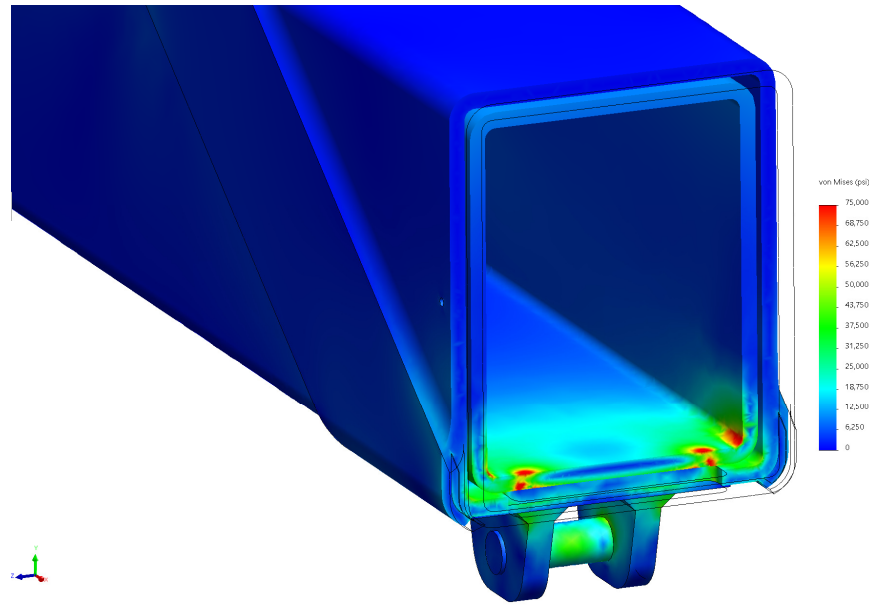


Figure 5b – Stress plot on mesh at end of tube #1

Successive section views through this area demonstrate that the reinforcing band improves overall stress in tube #1, but local concentrations from roller contact are still high, and tube #2 is not aided.





*Figure 5c – Three sections through same stress plot*

The bearing cassette system is key to success of this design concept. At the overlap between sections 2 and 3 the cassette and tube models were made more detailed. Virtual bolts were defined for all fasteners, in this case #10 socket cap screws with 10 ft-lb torque preload. Contact conditions are defined between bearings, bearing shafts, cassette frames, and the tubes.

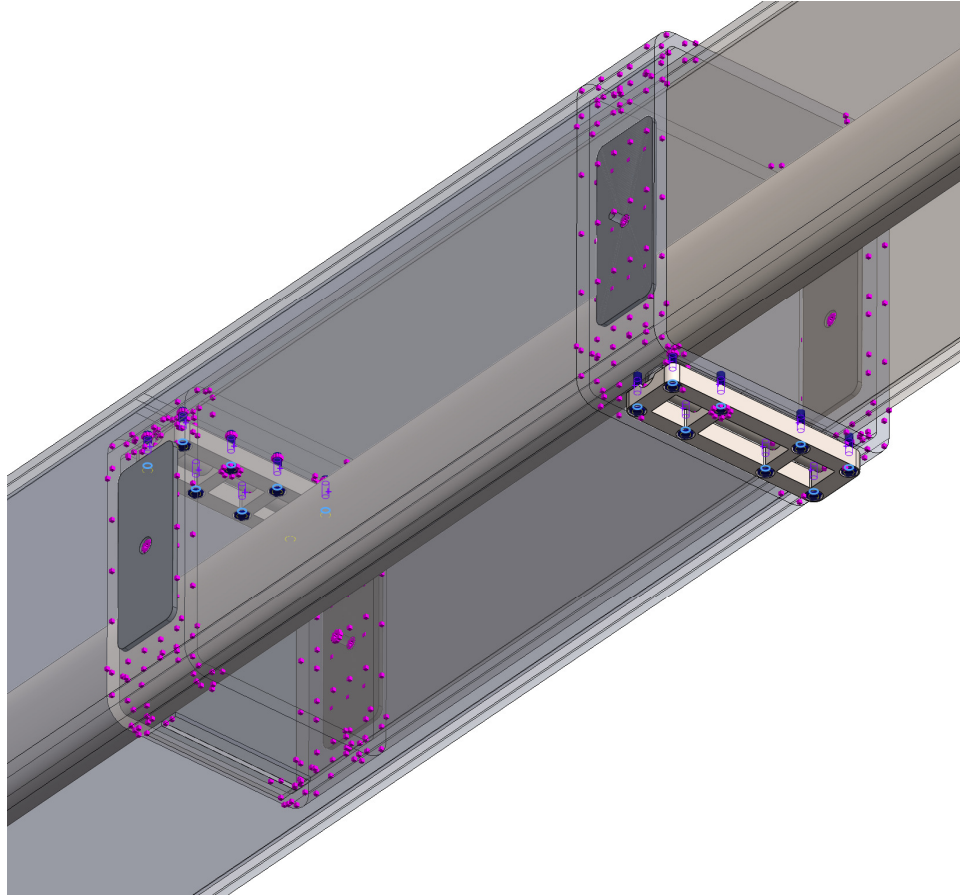


*Figure 5d – Model and simulation detail at 2-3 overlap*

The bearing models remain solid cylinders, sized just larger than the shaft. But here they float in free contact with the shaft and the retaining faces of the holder. A refined mesh improves capture of bending in the tube walls and fine stress gradients in the cassette frames.

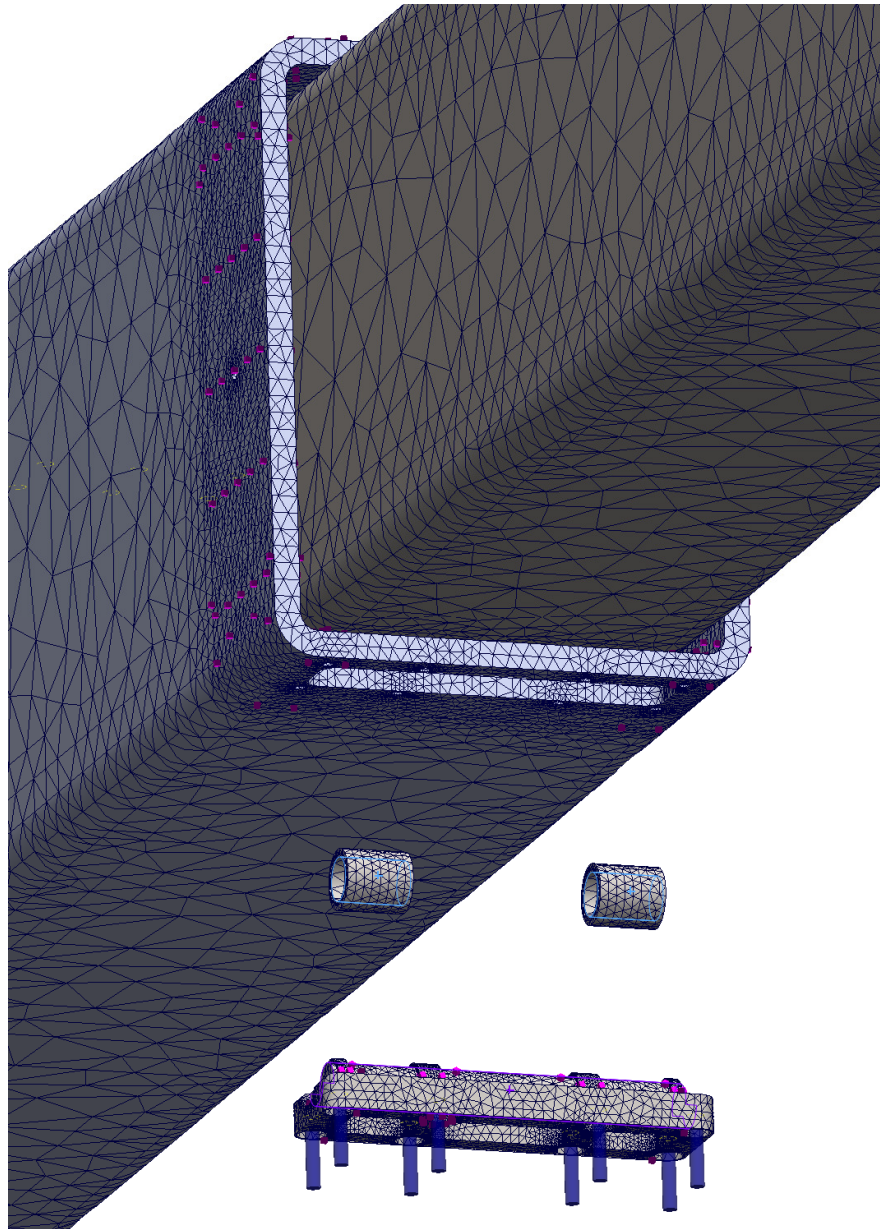


*Figure 5e – Mesh on exploded view at tube end*

Previously only net forces on the bearings have been considered. In this more detailed model local stresses can be investigated. A section view through this bearing cassette under load (boom extended, load vertical, minimum overlap) shows a condition seen to some extent in every location.

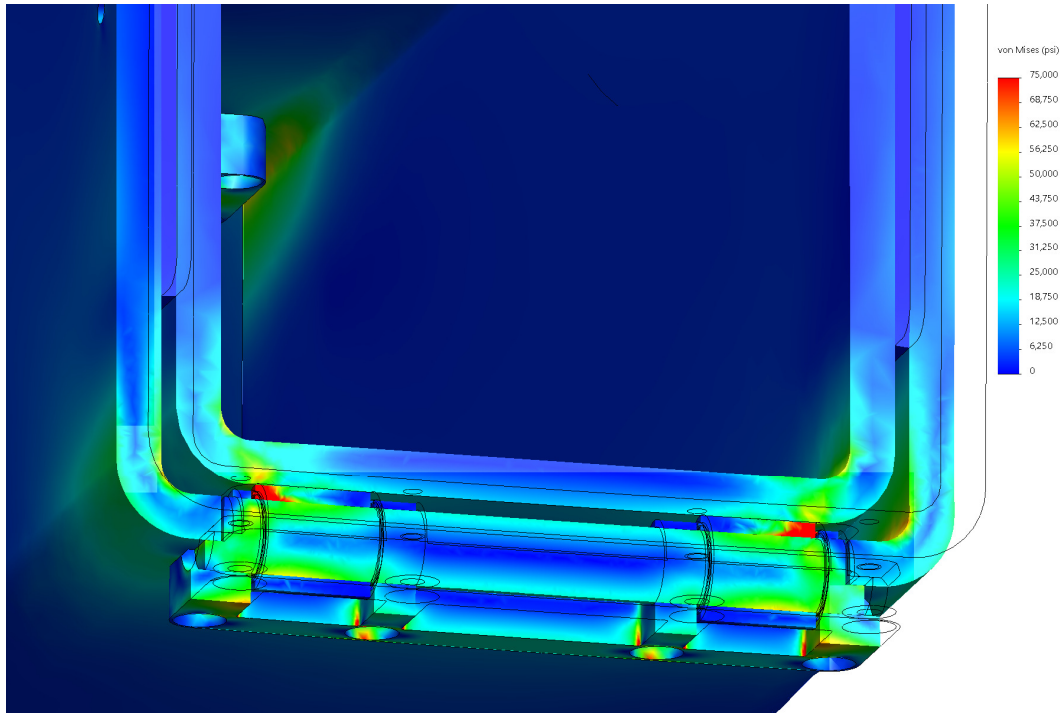


*Figure 5f – Section through stress field at bearing 2-3*

Stress in the bearing is concentrated at the outside edges. Magnification of the displacement reveals distortion of the relatively thin-walled tubes as the cause of this concentration.

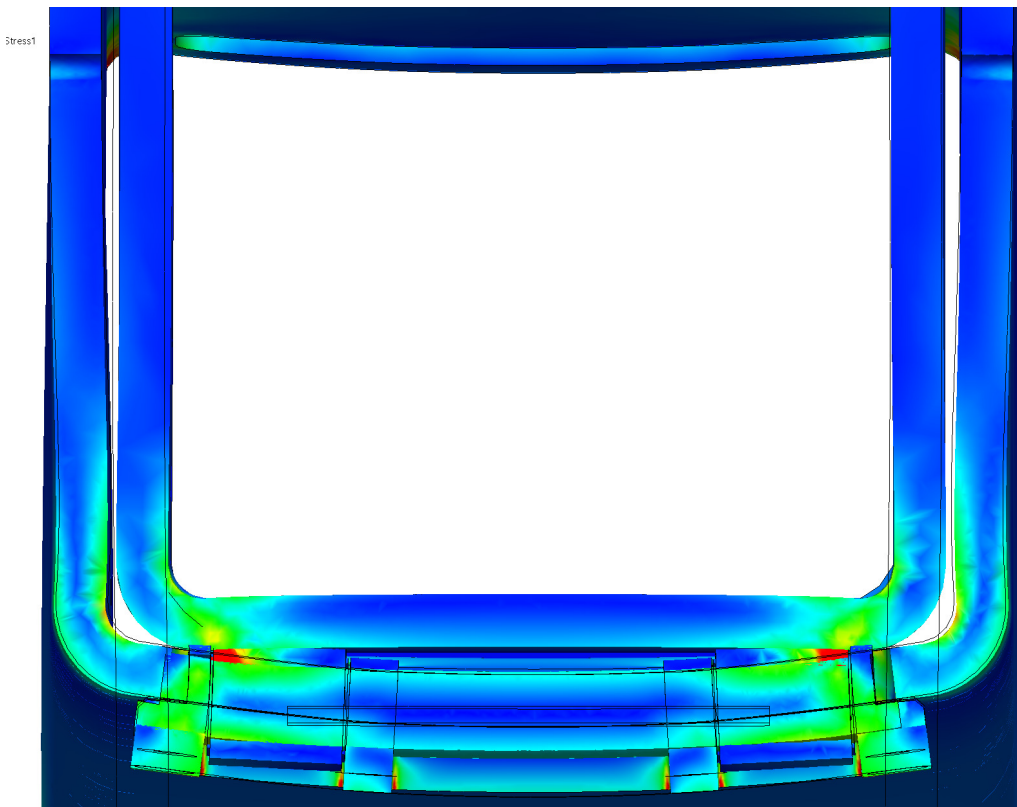


*Figure 5g – Stress through same section (10X displacement)*

The free end of tube #2, to which the bearing cassette is fastened, bows outward. The loaded section of tube #3 curves some in the opposite direction. The misalignment puts the outside edges of the bearing surfaces in much harder contact than the inside.

Fastener forces are taken from the bearing cassette frames. The forces exceed 3000 pounds in some instances.

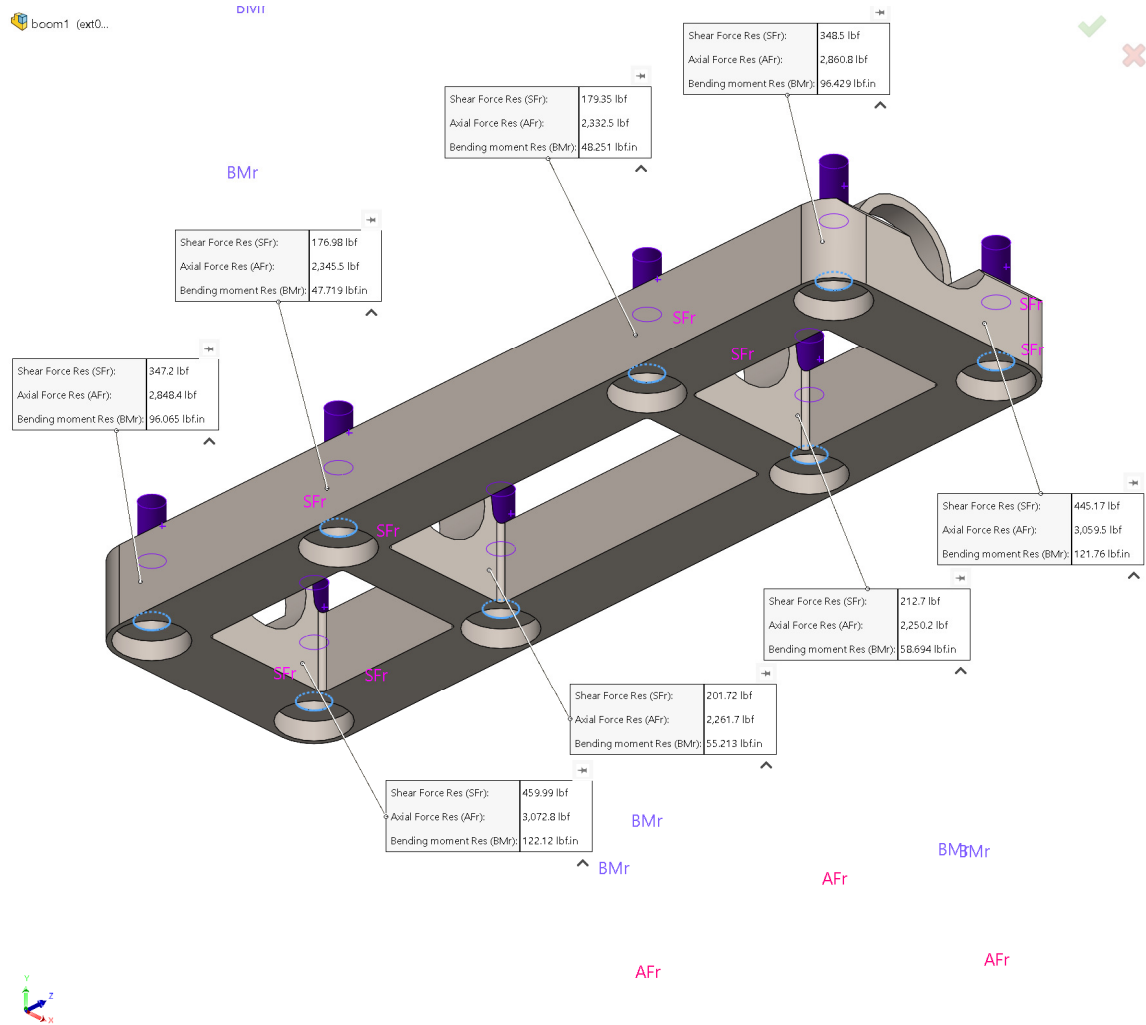
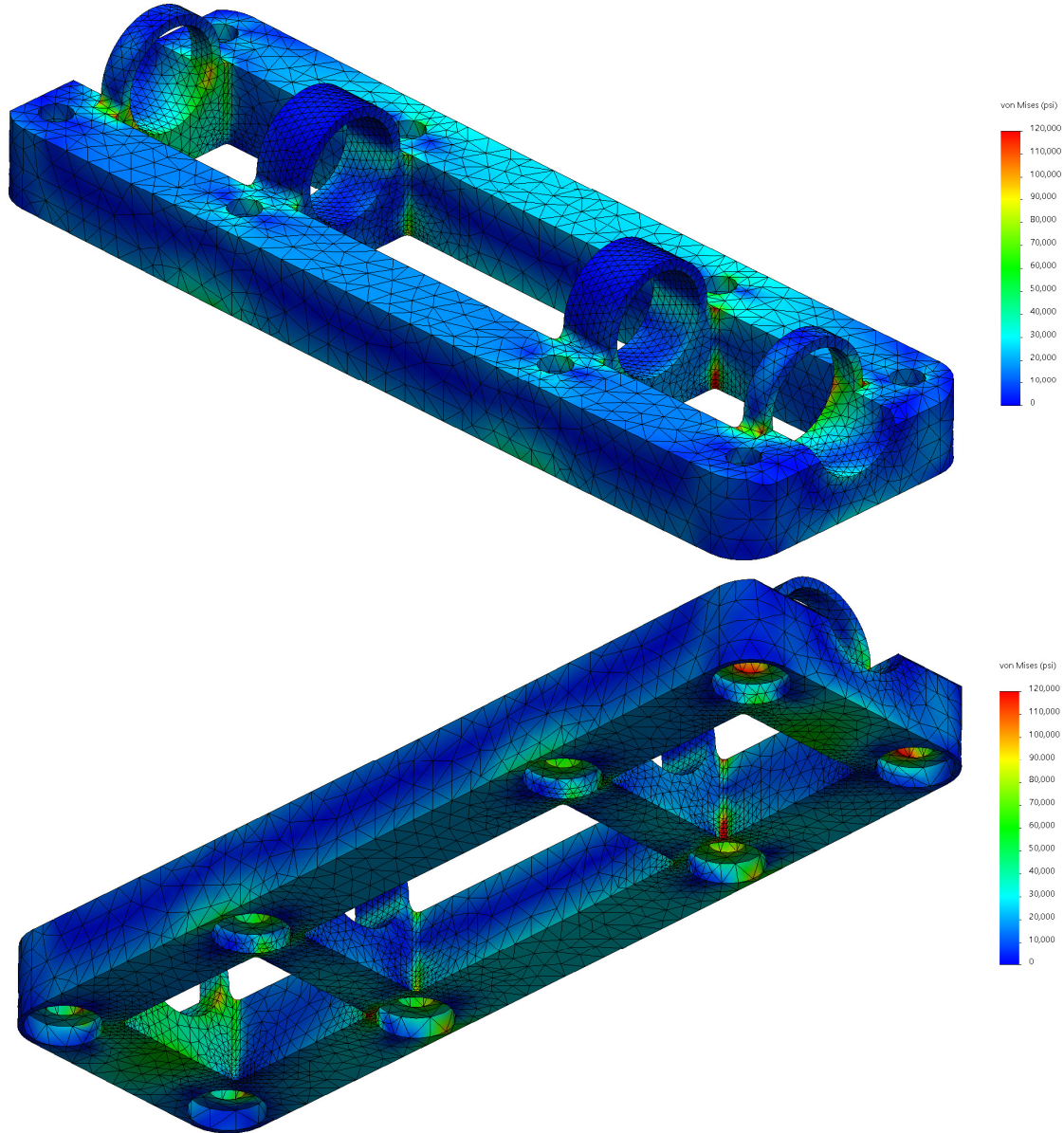


Figure 5h – Screw forces on bearing cassette

These forces are larger than the holding capacity of a high-strength #10 fastener. This is also more than the pullout force expected in threads through the steel tubes.

The cassette frame itself will be made from a high strength cast alloy.



*Stress plot (with mesh) on cassette frame at position*

Stress peaks are seen only at fine details and tight radii. Design of final as-cast geometry may address these locations.

## 6.0 Conclusion

The proposed reach boom design is conceptually valid, but not successful as currently sized and rated. As total moments between roller pairs increase from load end to operator end, local forces increase. Tube sections 1 and 2 could be made from thicker walled material.

Needle roller bearings are poorly suited to this application. Flex in the tube walls concentrates load on one edge of each bearing. For this low-speed application plain bearings with either limited self-alignment or crowned bearing surface may be investigated.

The cassette frames work well but are sized for fasteners that are too small in some locations. Tube wall thickness must also be increased in these locations to prevent thread pull out.

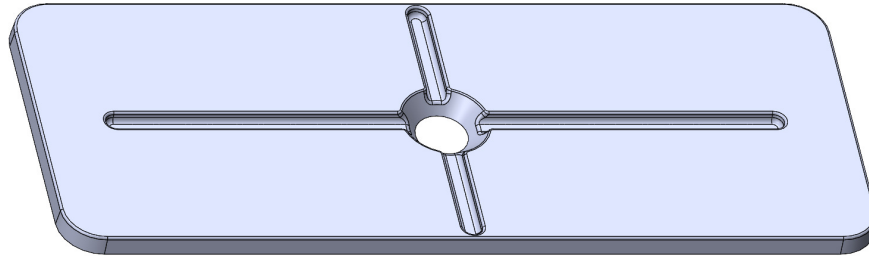
The sliding wear pads are rated for a relatively low PV. As these values are often generated against dry steel, and these pads have provision for lubrication, the PV may be very conservative. Consultation with the material provider and/or experimentation are recommended.

Hertzian contact stress against the tube sections cannot be estimated at this time. Flex in the tube walls leads to misalignment with the cylindrical roller bearings. If alignment can be ensured, these values can be calculated very accurately with handbook methods.

## APPENDIX

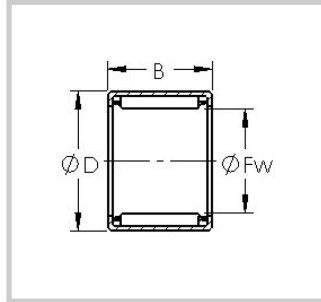
### Specified hardware:

The proposed wear pad has a load surface area of 8.4 square inches.



Its proposed material is Nylatron GSM with a limiting pressure-velocity of 3000 psi-ft/min. At 10 fpm this gives an allowable force of 2520 pounds.

The proposed roller bearings are the AST SCE912 (from tubes 4 to 3) and AST SCH1016 in all other locations.



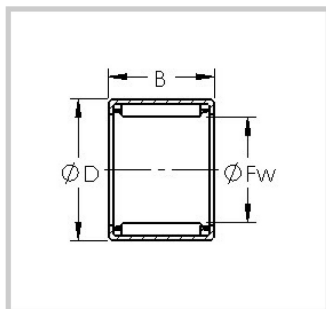
Part Number: SCE912 Inch Series Needle Roller Bearing



Product Details

Specifications

Bearing Type	Cage Retained Rollers	
Outer Dia (D)	0.7500	in
Width (B)	0.7500	in
Dynamic Load Rating (Cr)	2,410	lbs
Static Load Rating (Cor)	3,700	lbs
Max Speed (Grease)	19,600	rpm
Shaft (Fw)	0.563	in
Weight (g)	12.00	grams
Material	Drawn cup: Hardened carbon steel alloy, Rollers - 52100 Chrome steel or equivalent	



Part Number: SCH1016 Inch Series Needle Roller Bearing



Product Details

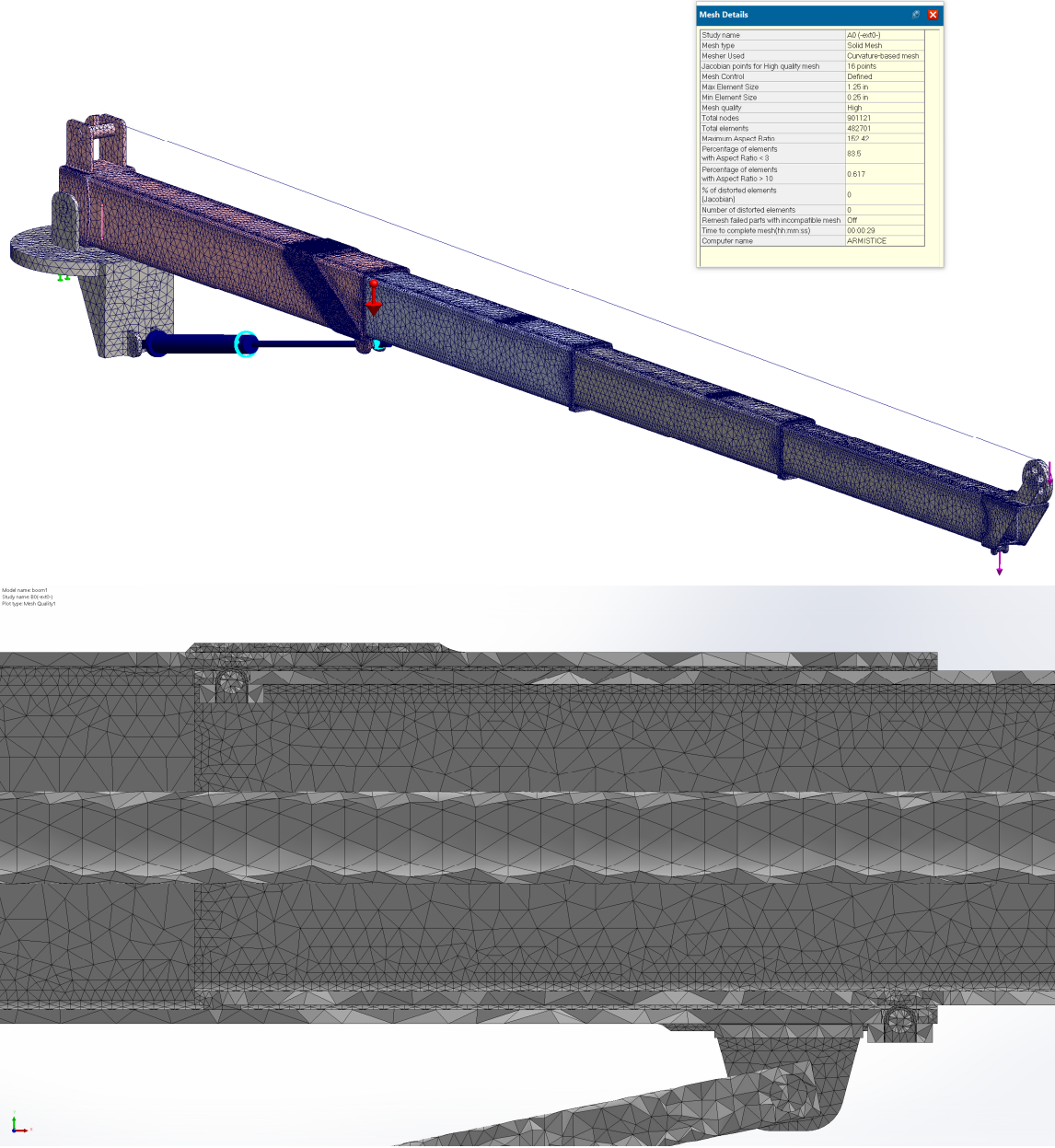
Specifications

Bearing Type	Cage Retained Rollers	
Outer Dia (D)	0.8750	in
Width (B)	1.0000	in
Dynamic Load Rating (Cr)	4,300	lbs
Static Load Rating (Cor)	6,300	lbs
Max Speed (Grease)	17,600	rpm
Shaft (Fw)	0.625	in
Weight (g)	25.00	grams
Material	Drawn cup: Hardened carbon steel alloy, Rollers - 52100 Chrome steel or equivalent	

Static load ratings are 3700 lbf for the SCE912 and 6300 lbf for the SCH1016.

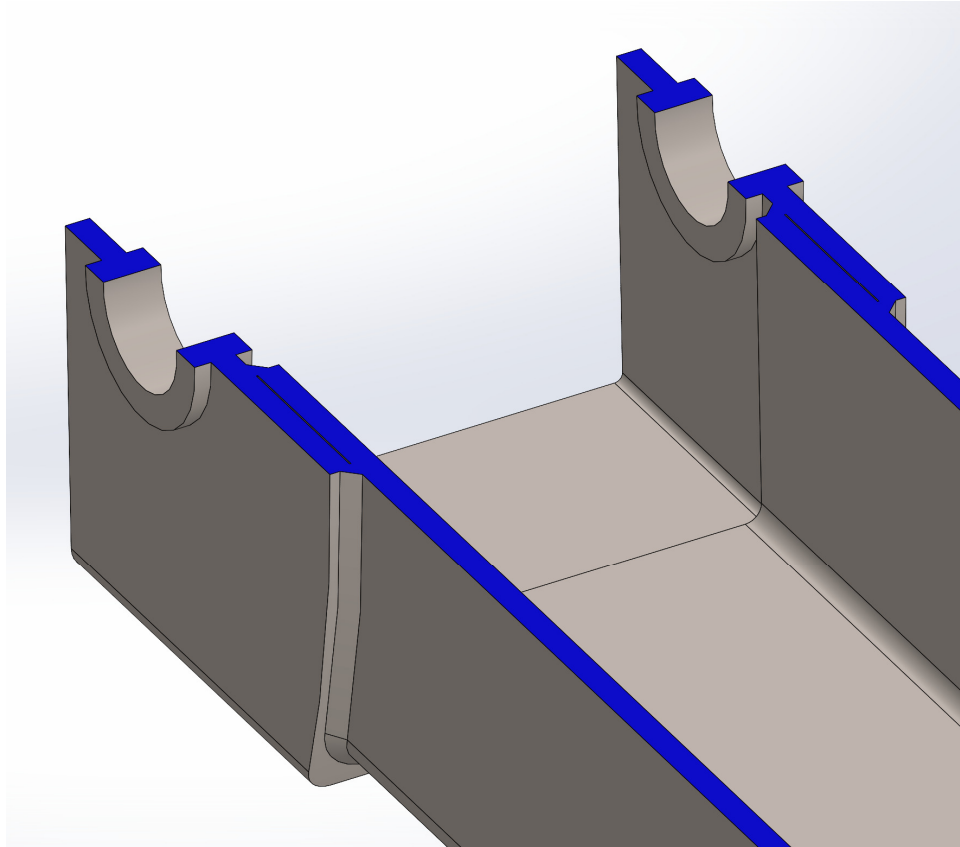
Analysis Setup:

Linear static finite element analysis is performed on a mesh of 2<sup>nd</sup>-order tetrahedrons. Local refinement is performed around areas of interest, curving geometry, or where high stress gradients are initially found. A typical mesh is shown, with its statistics – about 900,000 nodes on under 500,000 elements.



Typical run time is under 12 minutes on a late-model Intel i7-based workstation.

Weldments are treated as single solids. Welds are modeled literally in 3D CAD, with gaps maintained as expected based on typical penetration.



Loading for all runs is by gravity vector and applied loads at the hook end, load split 50/50 between front sheave and static hook. Offset loading is achieved by angling the vectors.

The only fixture is at the underside of the simplified base model.

The lift cylinder is modeled as live steel elements, with “pin” connectors at either end and between the piston and shell. This permits free movement of the cylinder in every degree except its length.

No-penetration contact is defined between rollers and tubes, and between the wear pads and sliding tubes. The pad locating system is assumed effective and the pads are bonded to the non-sliding tubes.

A “pin connector” defines location and free motion of the load end cable sheave. A rigid link defines the cable from motor reel to load end sheave.

## Complete Force Results:

Output force values for every contact location are tabulated below. Forces in excess of hardware ratings are highlighted.

STUDIES						ROLLERS												PADS											
study	load angle	cut length	overlap	lift angle	load (lb)	2 to 1		1 to 2		3 to 2		2 to 3		4 to 3		3 to 4		2 to 1		1 to 2		3 to 2		2 to 3		4 to 3		3 to 4	
						left	right	left	right	left	right	left	right	left	right	left	right	left	right	left	right	left	right	left	right	left	right	left	right
A0	0	72	20	0	1600	8090	8111	9194	9199	5136	5160	6127	6136	2499	2494	3377	3388	2257	2267	1974	1983	1792	1789	1479	1480	858	858	1096	1098
A1	0	72.75	21	0	1600	7626	7641	8729	8736	4820	4881	5827	5843	2351	2353	3236	3240	2146	2146	1950	1955	1699	1691	1419	1421	810	808	1047	1048
A2	0	73.5	22	0	1600	7210	7229	8321	8322	4580	4593	5564	5581	2219	2230	3113	3110	2071	2082	1948	1932	1607	1613	1364	1365	767	764	1026	1021
A3	0	74.25	23	0	1600	6839	6844	7941	7951	4335	4355	5337	5319	2110	2104	2992	2996	1934	1939	1925	1924	1509	1509	1294	1299	735	735	981	988
A4	0	75	24	0	1600	6478	6510	7593	7607	4135	4111	5109	5115	2005	1993	2887	2885	1851	1849	1906	1902	1449	1438	1242	1242	698	697	935	938
B0	15	72	20	0	1600	8285	7365	8502	9267	5259	4688	5637	5310	2548	2276	3055	3480	4889	418	7879	5061	3516	646	134	3504	1778	335	379	2276
B1	15	72.75	21	0	1600	7826	6920	8040	8828	4943	4426	5344	5927	2408	2136	2920	3335	4615	407	7932	4781	3312	597	137	3346	1672	308	362	2172
B2	15	73.5	22	0	1600	7410	6539	7639	8439	4710	4151	5099	5668	2285	2013	2806	3205	4415	426	29	4563	3141	590	144	3205	1568	286	363	2093
B3	15	74.25	23	0	1600	7039	6178	7276	8075	4474	3920	4890	5413	2168	1902	2693	3091	4151	378	86	4430	2956	534	138	3068	1506	289	357	2036
B4	15	75	24	0	1600	6687	5864	6949	7740	4255	3712	4686	5192	2063	1800	2594	2984	3935	362	156	4298	2820	519	122	2925	1429	275	333	1944
C25	0	72	20	25	1732	7795	7826	8854	8873	4971	4970	5909	5943	2413	2407	3271	3274	2232	2228	1964	1971	1771	1770	1446	1445	830	830	1065	1063
C40	0	72	20	40	1990	7670	7709	8665	8700	5004	4999	5905	5912	2543	2534	3366	3374	2181	2181	1951	1948	1758	1765	1433	1435	891	894	1085	1083
C55	0	72	20	55	2550	6788	6805	7685	7702	4347	4347	5179	5181	2072	2060	2843	2842	1952	1951	1695	1683	1550	1548	1282	1283	726	728	940	939
C55-4	0	75	24	55	2550	5561	5577	6474	6478	3593	3595	4435	4433	1758	1756	2353	2541	1602	1600	1630	1635	1269	1274	1089	1091	617	617	825	828